Journal of Zhejiang University SCIENCE
ISSN 1009-3095
http://www.zju.edu.cn/jzus
E-mail: jzus@zju.edu.cn

Application of electrical capacitance tomography for imaging industrial processes

DYAKOWSKI Tom

(*School of Chemical Engineering and Analytical Science, The University of Manchester, Manchester M60 1QD, UK*)

E-mail: t.dyakowski@manchester.ac.uk

Received Aug. 26, 2005; revision accepted Sept. 10, 2005

Abstract: Electrical tomography is, in certain cases, the most attractive method for real imaging of industrial processes, because of its inherent simplicity, rugged construction of the tomographer and high-speed capability. This paper presents examples illustrating applications of electrical tomography for imaging fluidized beds, bubble columns and pneumatic conveyors. Electrical tomography opens up new ways for processing, imaging and modelling multi-phase flows as shown by 2D and 3D images illustrating the various types of flow morphology.

Key words: Electrical tomography, Fluidization, Pneumatic conveying, Bubble columns
doi:10.1631/jzus.2005.A1374 **Document code:** A **CLC number:** TB126

INTRODUCTION

In recent years, developments in the technology have led to widespread use of electrical tomography for industrial applications. Electrical tomography is based on the use of an array of the sensors located along the pipe axis or the reactor circumference. Images obtained from electrical tomography show the cross-sectional spatial variation of dielectric constant or resistivity. With proper calibration these images depict the distribution of phase density or phase concentration in the process. These are vital for understanding the complex interaction between flowing phases.

Cross-section slices can be applied to distinguish between different flow regimes or to measure some specific flow characteristics characterizing non-homogeneous phase distribution (Williams and Beck, 1995). They can also be used to validate various flow models applied in computational fluid dynamics or to construct the constitutive equations describing interactions between flowing phases as discussed below. Here various approaches in processing tomographic data will be illustrated for both gas/solids and gas/liquid systems.

PHASE DISTRIBUTION WITHIN ACIRCULATING FLUIDIZED BED

The circulating fluidized bed apparatus used in the experiment is described in (Dyakowski *et al*., 1997). The capacitance tomographic images were obtained using an 8 electrodes single plane capacitance sensor with driven guard electrodes. The images will correspond to the contents of a finite volume defined by the height of sensing electrodes and pipe diameter. This is an inherent feature of an ECT taken along the electrode height. For flow in the riser, the data from ECT measurements were reconstructed onto a square grid, which has size 32 by 32 pixels. A sequence of instantaneous images is shown in Fig.1.

The images show that the solids concentrations is 2% to 12%, the flow rate is annular in character, a region of high solids concentration flow near the pipe wall and a region of low solids concentration flow near the centre of the pipe. A time averaged image, obtained from a thousand instantaneous images, over a period of 10 s, is shown in Fig.2.

In contrast to the instantaneous images, the average solids distribution exhibits a higher degree of axial symmetry. For a three dimensional and non-sta-

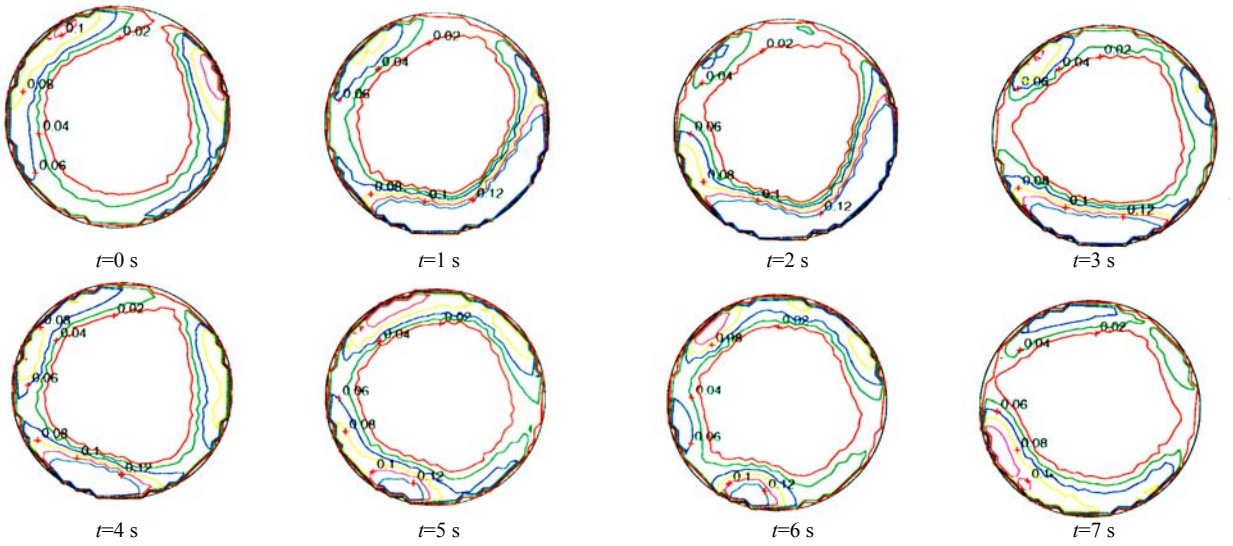

Fig.1 Instantaneous solids distribution profiles

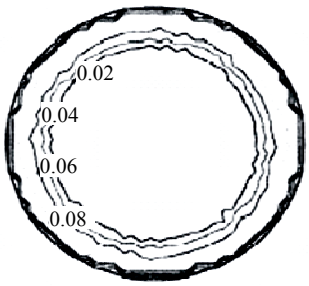

Fig.2 Time average solids distribution profile

tionary multiphase flow, it will be modelled by composite-average equations. These are based on the space/time or time/space averaging operators. For a two-phase flow, the following formula expresses the equivalence between the two types of operators:

$$\frac{1}{A}\iint_A\left[\frac{1}{T}\int_T X(r,t)\mathrm{d}t\right]\mathrm{d}A=\frac{1}{T}\int_T\left[\frac{1}{A}\iint_A X(r,t)\mathrm{d}A\right]\mathrm{d}t \quad (1)$$

where symbols A and dA refer to the cross sectional area, T and dt refer to the time interval. This equation simply implies that the same information (in an average sense) can be obtained in two ways. The first way is to perform a set of measurements by a local probe inserted into the flow. Here, the sensor would have to be traversed through all point in the space domain and each individual measurement would have to last a representative period. The second way is to perform "cross-sectional" measurements (such as tomographic) over a single period T. It is clear that the latter represents a more effective method of investigating complex processes.

Pugsley *et al*.(2003) studied the dynamics of gas/solids flow within a circulating fluidized riser with an internal diameter of 14 cm. The experimental results were obtained for a mixture of placebo pharmaceutical granules with particle density of 1.1 g/cm^3 and particle size ranging from 40 μm to greater than 3 mm in diameter. They validated the results from the ECT system by comparing the reconstructed images to the images obtained from a fibre optic probe. This study showed that the time-averaged results from both imaging techniques (as shown in Fig.3) are in agreement for the bubbling mode for gas superficial velocities above 0.25 m/s. The authors state that their findings are consistent with earlier results (Dyakowski *et al*., 1997), showing that the ECT system works better in dense beds. On the other hand, the instantaneous measurements obtained by both techniques show poor agreement, which the authors suggest might be caused by the difference in measured volumes: 0.002 cm^3 for the optical fibre and 0.77 cm^3 for the ECT. The volumes through which capacitance measurements were taken are much larger than the voxel volume, but it should be emphasised that the voxel size does not affect the accuracy of the reconstructed image. For a given electrode arrangement, the number and size of voxels can be varied somewhat independently of the number and size of

electrodes. Therefore, the special resolution is mainly a function of the geometry of the electrodes as discussed by Wang (1998).

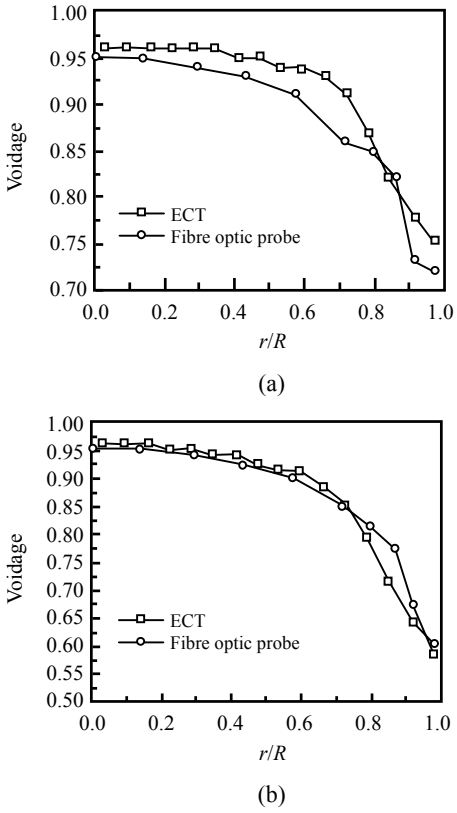

Fig.3 Comparison of radial voidage profiles measured with ECT and fibre optic probe in the circulating fluidised riser containing FCC catalyst (diameter 80 μm) (Pugsley *et al*., 2003). (a) Riser solids mass flux 148 kg/(m^2·s) and superficial gas velocity 4.7 m/s; (b) Riser solids mass flux 264 kg/(m^2·s)

Bubble diameters and rise velocities within a bubbling fluidized bed have been measured by Halow and Nicoletti (1992), Halow *et al*.(1993), Wang *et al*.(1995), Makkawi and Wright (2004), White (2003), and McKeen and Pugsley (2003). Knowledge of these two parameters is critical for a better modelling of gas-solids interactions as discussed by McKeen and Pugsley (2003). The authors claim that predictions from their modified two-fluid model are in good agreement with experimental results.

The application of an ECT system for imaging gas-solids flow patterns within a dipleg was discussed by Wang (1998). The results showed that solids falling down from a cyclone distribute themselves into an annular shape around the wall of the dipleg and also into the centre of the dipleg. Except for the region near the wall, the time and cross-sectional average solids volume fraction distributions compared well with those obtained from the literature correlations as shown in Fig.4.

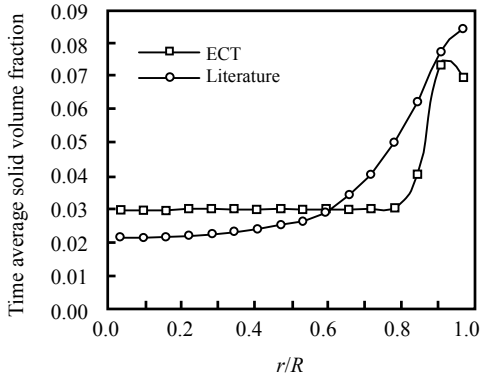

Fig.4 Comparison of time average solids distribution with the literature data (Wang, 1998) solids mass flux 225 kg/(m^2·s)

PHASE DISTRIBUTION WITHIN BUBBLE COLUMN

George *et al*.(2000) studied the dynamics of gas/liquid churn-turbulent flows in a vertical column with an inner diameter of 19 cm. The measurements were taken at a distance of 97 cm from the gas inlet. Variations in conductivity were minimised by keeping the liquid at a nearly constant temperature (±0.2 °C). Churn-turbulent measurements were taken for five gas flow rates (420, 830, 1250, 1670 and 2500 cm^3/s) through a vertical column filled with water; the corresponding superficial gas velocities were within the range of 1.5 to 8.8 cm/s. The results from electrical tomography were compared with gamma-densitometry tomography measurements. An example of the comparison of time averaged gas volume fractions between these two techniques is shown in Fig.5. The authors claim that the average cross-sectional values and radial profiles from both methods agreed to within 1% of gas void fraction. Such a good agreement was achieved despite the large difference in collection times for both methods (about 23 min for gamma tomography but less than 20 s for electrical tomography).

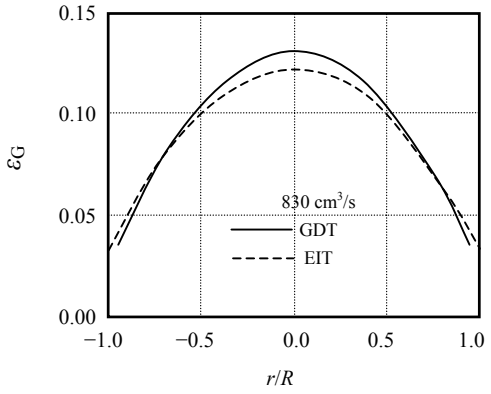

Fig.5 Comparison of symmetric radial gas volume fraction profiles from gamma densitometry tomography and electrical tomography; gas volume flow rate 830 cm^3/s (George *et al*., 2000)

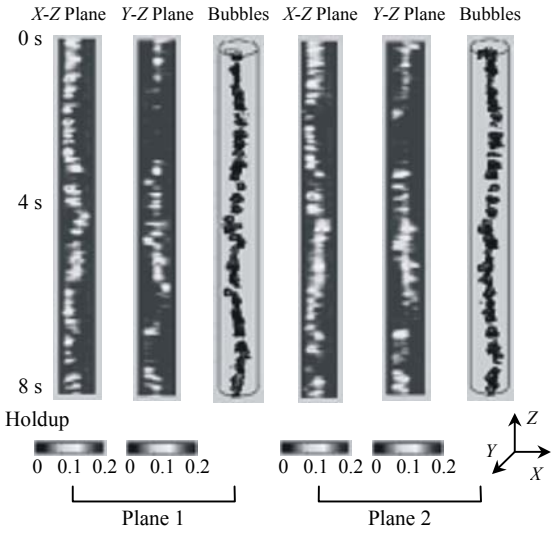

Fig.6 The effect of air velocity on the bubble size and trajectory for bubbles ascending through Norpar 15 as discussed in Warsito and Fan (2001; 2003)

Successive imaging frames, taken at a single level, represent how the phase distribution varies with time at a particular location. Assuming that the investigated fluid is flowing with constant velocity along the channel axis while the measurements are taken, a 3D representation of the phase distribution can be constructed. This can be done either in an arbitrary scale or by relating the scale to the product of fluid velocity and imaging time. The latter needs a method of measuring fluid velocity, which can be obtained, for example, from a twin-plane tomographic system.

The effect of air velocity and the presence of solids on a 3D air bubble flow structure in a gas liquid column were studied by Warsito and Fan (2001; 2003). The results were obtained for two types of dielectric fluids (Norpar 15 and Paratherm) and polystyrene beads whose permittivity is close to that of Paratherm. The measurements were taken from a vertical column of 0.1 m internal diameter and 1 m height. The gas distributor was a single nozzle with a diameter of 0.5 cm. A twin-plane sensor using 12 electrodes for each plane was applied and the distance of plane 1 and plane 2 from the distributor was 10 cm and 15 cm, respectively. A modified Hopfield dynamic neural network algorithm was applied for data reconstruction.

The effect of air velocity on the bubble break-up and coalescence, for Norpar 15, is shown in Fig.6. The authors conclude that for smaller bubbles the tomograms provide information on the amount of the dispersed phase (solids concentration or gas voidage, or gas hold-up within a gas-liquid system).

3D flow structures based on tomographic measurements can be validated by using photographs as discussed elsewhere (Jaworski and Dyakawski, 2001). Of course, on the fundamental level, the information obtained from the flow visualisation (photographs) is different from that obtained by combing tomographic images. Whereas the photographs show the spatial information at a given instant, the tomographic results represent the temporal changes at a given spatial location (that of the sensor). The two approaches would be equivalent only if the flow structures were "frozen" while moving along the pipe. Although this is not necessarily true, it is worth noting the apparent similarities between the photographs and the tomographic data. Of course, using a twin-plane tomographic system allows obtaining the time delay between the appearance of slugs in respective planes and therefore the propagation velocity of slugs. The length of the slug can then be calculated as the time that the slug was present on one of the planes multiplied by the propagation velocity. It is apparent that, despite difficulties encountered in the ECT system measurements (reconstruction algorithm errors, averaging along the electrodes), the technique can provide unique information about the structure and evolution of three-dimensional and unsteady gas-solids flows.

A photograph and constructed image of the slug

of solids during a dense mode of conveying system is shown in Fig.7. One of the methods used to extract sharp boundaries between the phases from the ECT images is the so-called "thresholding" as discussed in (Dyakowski *et al*., 1997).

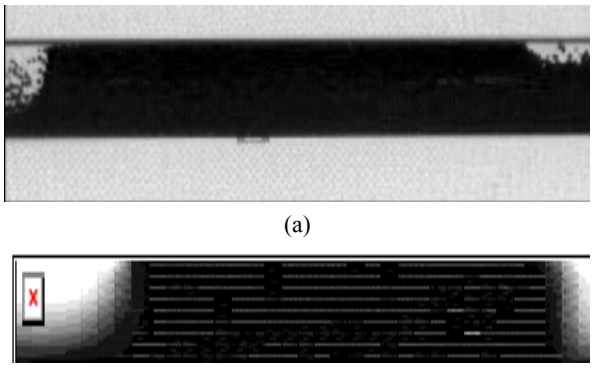

Fig.7 (a) High speed camera visualization of the slug flow in horizontal pipe; (b) The longitudinal cross-section of the slug flow obtained from tomograms. The data were obtained by extracting pixels from the vertical axis of each tomogram and combining them as a time series (Jaworski and Dyakowski, 2001)

CONCLUSION

This short review describes the latest progress made with applications of electrical tomography for imaging various types of industrially important processes. The concept of distributed sensor and measurement protocol controlled by a computer is the main ingredient of electrical tomography. Images illustrating the distribution of electrical properties are obtained by solving ill-posed inverse problem.

As described, electrical tomography opens up new ways for processing, imaging and modelling multi-phase flows as shown by 2D and 3D images illustrating the various types of flow morphology. Future work will focus on applying tomographic techniques for process control.

References

Dyakowski, T., Edwards, R.B., Xie, C.G., Williams, R.A., 1997. Application of capacitance tomography to gas-solids flows. *Chemical Engineering Science*, **52**:2099-2110.

George, D.L., Torczynski, J.R., Shollenberger, K.A., O'Hern, T.J., Ceccio, S.L., 2000. Validation of electrical-impedance tomography for measurements of material distribution in two-phase flows. *International Journal of Multiphase Flow*, **26**:549-581.

Halow, J.S., Nicoletti, P., 1992. Observation of fluidized bed coalescence using capacitance imaging. *Power Technology*, **69**:255-277.

Halow, J.S., Fasching, G.E., Nicoletti, P., 1993. Observation of a fluidized bed using capacitance imaging. *Chemical Engineering Science*, **48**:643-659.

Jaworski, A.J., Dyakowski, T., 2001. Application of electrical capacitance tomography for measurement of gas-solids flow characteristics in a pneumatic conveying system. *Measurement Science and Technology*, **12**:1-11.

Makkawi, Y.T., Wright, P.C., 2004. Tomographic analysis of dry and semi-wet bed fluidization: the effect of small liquid loading and particle size on the bubbling behaviour. *Chemical Engineering Science*, **59**:201-213.

McKeen, T., Pugsley, T., 2003. Simulation and experimental validation of a freely bubbling bed of FCC catalyst. *Powder Technology*, **129**:139-152.

Pugsley, T., Tanfara, H., Malcus, S., Cui, H., Chaouki, J., Winters, C., 2003. Verification of fluidized bed electrical capacitance tomography measurement with a fibre optic probe. *Chemical Engineering Science*, **58**:3923-3934.

Wang, S.J., 1998. Measurement of Fluidization Dynamics in Fluidized Beds Using Capacitance Tomography. Ph.D Thesis, UMIST, Manchester, UK.

Wang, S.J., Dyakowski, T., Xie, C.G., Williams, R.A., Beck, M.S., 1995. Real time capacitance imaging of bubble formation at the distributor of a fluidized bed. *Chemical Engineering Science*, **56**:95-100.

Warsito, W., Fan, L.S., 2001. Measurement of real-time flow structures in gas-liquid and gas-liquid-solid flow systems using electrical capacitance tomography (ECT). *Chemical Engineering Science*, **56**:6455-6462.

Warsito, W., Fan, L.S., 2003. ECT imaging of three-phase fluidized bed based on three-phase capacitance model. *Chemical Engineering Sciences*, **58**:823-832.

White, R.B., 2003. Using Electrical Capacitance Tomography to Investigate Gas Solid Contracting. Proceedings of 3rd World Congress on Industrial Process Tomography, Banff, Canada, p.840-845.

Williams, R.A., Beck, M.S., 1995. Process Tomography —Principles, Techniques and Applications. Butterworth-Heinemann, Oxford, UK.